

Electrical activity of multivacancy defects in silicon

P. Santos^{*1}, J. Coutinho¹, M. J. Rayson², and P. R. Briddon³

¹ Department of Physics & I3N, University of Aveiro, Campus Santiago, 3810-193 Aveiro, Portugal

² Department of Engineering Sciences and Mathematics, Luleå University of Technology, 97187 Luleå, Sweden

³ School of Electrical, Electronic and Computer Engineering, Newcastle University, Newcastle Upon Tyne NE1 7RU, United Kingdom

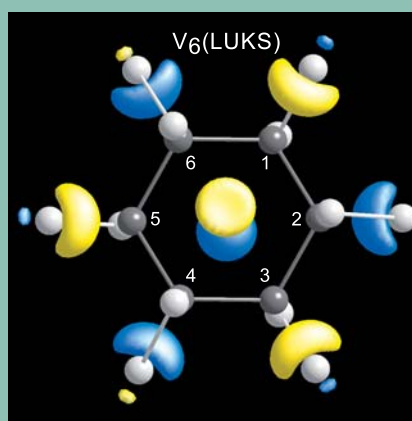
Received 23 April 2012, revised 17 May 2012, accepted 17 May 2012

Published online 24 August 2012

Keywords silicon, vacancies, radiation effects, electrical levels

* Corresponding author: e-mail: paulodsantos@ua.pt, Phone: +351-234247051, Fax: +351-234378197

The formation processes and properties of multivacancy defects in Si have been recently the subject of several research studies. Here we report on density functional calculations concerning the stability and electrical activity of the tetravacancy, pentavacancy and hexavacancy complexes in Si. Formation energy calculations indicate that Four-Fold Coordinated (FFC) V_4 and V_5 are more stable than Part-of-Hexagonal-Ring (PHR) or planar structures by at least 1.2 eV and 0.6 eV, respectively. This relative stability order between configurations remains unchanged for different charged states from double plus to double minus. Calculations of the electrical activity predict deep acceptor levels for the FFC defects. Accordingly, electron traps related to $(-/0)$ and $(= /-)$ levels near $E_c - 0.5$ eV were found for V_4 and V_5 , whereas levels for V_6 were estimated at $E_c - 0.35$ eV. No donor levels were found for these defects.



Lowest Unoccupied Kohn-Sham (LUKS) level of a hexavacancy (V_6) in silicon. White and black (numbered) atoms represent Si and vacant sites, respectively.

© 2012 WILEY-VCH Verlag GmbH & Co. KGaA, Weinheim

1 Introduction The degradation of silicon detectors when exposed to several types of radiation is a significant issue in particle detection applications such as medical imaging or in fundamental science including high-energy physics [1]. This degradation is related to the electrical activity of some structural point defects like vacancies or interstitial atoms (and their related aggregates), which are a direct product of the exposure to a radiation source. This is the case of the single Si vacancy (V) [2], and also of some small multivacancy clusters [3].

Early Electron Paramagnetic Resonance (EPR) and annealing studies by Lee and Corbett [3] established a connection between specific paramagnetic signals and the production, transformation and disappearance tempera-

tures of the simplest vacancy clusters. The levels of the most elemental vacancy aggregate – the divacancy – were also early established. From Deep Level Transient Spectroscopy (DLTS), we know that in n-type Si it produces two prominent peaks related to first and second acceptor levels at $E_c - 0.42$ eV and $E_c - 0.23$ eV [4], whereas in p-type material it has a hole trap related to a donor level at $E_v + 0.20$ eV [5]. For a long period of time the electrical activity of the trivacancy and larger vacancy clusters was a matter of speculation, and much of the work relied on the above mentioned EPR data. More recently, concurrent work at Brunel [6] and at CERN [7] unveiled the first leads for the electrical activity of larger vacancy complexes. Accordingly, two deep electron traps at $E_c - 0.45$ eV and

$E_c - 0.35$ eV were linked to the Si trivacancy and another trap at $E_c - 0.37$ eV was tentatively connected to the Si tetravacancy (V_4). Their activation barriers for annealing out of about 1 eV are slightly smaller than the 1.4 eV barrier for migration of V_2 [8], and since the divacancies anneal out by being trapped at donors or oxygen upon diffusion (and not by capturing mobile interstitial impurities), it is likely that the measured barriers correspond to migration or rearrangement mechanisms.

Structural and electrical properties of small vacancy aggregates in Si are still a subject of debate. The *traditional* atomic models for these defects comprise a family referred as *Part-of-Hexagonal-Ring* (PHR) structures [9], where a given V_n complex (with $n \leq 6$), is obtained by placing $6 - n$ Si atoms at the vacant sites of a hexavacancy. The latter is obtained by removing an hexagonal ring of Si atoms in the lattice. This is depicted in Figs. 1(a)-(d), where V_5 and V_4 have respectively one and two additional Si atoms (shown in green) when compared to V_6 . Of special relevance is the fact that in V_6 all 12 Si dangling bonds that result from atom removal, reconstruct pairwise to form 6 long bonds [see green bonds in Fig. 1(b)], conferring to this defect great stability, and according to previous calculations [10, 11], no electrical activity. Conversely, PHR complexes possess highly reactive under-coordinated Si radicals (green atoms), responsible for two dangling bonds and higher formation energies [9].

More recently, alternative and more stable configurations for V_n ($3 \leq n \leq 5$) were proposed by Makhov and Lewis [12]. In this configurations, the $6 - n$ Si atoms in excess to those in V_6 are displaced towards interstitial positions, in a way that each of them binds to four Si radicals edging the hexavacancy cage. These are shown in Figs. 2(c) and 2(d) for the cases of V_5 and V_4 , respectively, where *green* Si atoms saturate four and eight dangling bonds around the hexagonal vacant ring, respectively. Analogously to V_6 , the remaining dangling bonds form long Si-Si reconstruction pairs. These configurations are known as *Four-Fold-Coordinated* (FFC) and formation energies of FFC V_3 , V_4 and V_5 were found below those of PHR counterparts by 0.6 eV, 1.1 eV and 0.7 eV, respectively. Also importantly, all FFC defects were predicted to be electrically inert. This picture was supported by the four-fold coordination of all atoms, but it is now clashing with the DLTS data assigned to V_3 and V_4 electron traps in n-type Si [6, 7].

Actually in the case of the trivacancy, recent DLTS measurements combined with density functional calculations demonstrated that FFC V_3 is in fact electrically active with an acceptor level at $E_c - 75$ meV [13]. This paper is especially relevant as it shows that both PHR and FFC V_3 defects are formed, the transformation between them can be cycled upon annealing and current injection treatments, but also suggests that larger FFC complexes could be electrically active as well. This bi-stability of V_3 is only possible if there are high enough barriers preventing de-

fect transformation above room temperature. We note however that the existing calculations indicate that the transformation barrier that separates V_5 (FFC) from V_5 (PHR) is estimated to be about 20-30 meV only [12], and unlike V_3 (PHR) the V_5 (PHR) structure should not hold at room temperature with the FFC structure being readily formed. These are among the issues that we want to address in this paper, and this can only be done by scrutinizing the charge-dependent stability and the electrical activity of these complexes.

2 Method We employed a computer implementation of the density-functional theory (AIMPRO), along with the local spin density approximation (LSDA) for the exchange and correlation potential. The explicit treatment of Si core states ($1s^2 2s^2 2p^6$) was avoided by using the Hartwigsen-Goedecker-Hutter pseudopotentials [14]. The Kohn-Sham states were expanded using a Cartesian-Gaussian basis set comprising 28 independent s-, p- and d-like orbitals per atom, whereas the charge density and potential terms are Fourier transformed using a plane-wave basis with a cut-off of 80 Ry. Cubic supercells comprising $512 - n$ atoms were employed in order to model V_n multivacancy clusters, and the Brillouin zone was sampled at $\mathbf{k} = \Gamma$. All atoms were allowed to moved along their forces with help of a conjugate gradient relaxation algorithm to minimize the energy. This was carried out until total energy and atom position changes dropped below 0.3 meV and 5×10^{-5} Å, respectively. Under these conditions, the lattice constant and bulk modulus of Si were respectively $a = 5.3947$ Å and $B = 98.3$ GPa, in good agreement similar calculations and with the experimental values.

For a V_n multivacancy in a periodic supercell of Si atoms, its formation energy E_f in the neutral charge state is simply

$$E_f[V_n] = E[V_n] - (N - n)\mu_{\text{Si}}, \quad (1)$$

where $E[V_n]$ is the total energy of the defective supercell made of $N - n$ atoms, and μ_{Si} the chemical potential of Si taken as the energy per atom from a pristine supercell made of $N = 512$ Si atoms.

Transition energies $E_d(q/q+1)$ of defects between two charge states q and $q + 1$, are measured in DLTS and can be estimated using the *marker method* [15]. This is done by comparing (off-setting) ionization energies and electron affinities of defective supercells, $I(q/q + 1) = E[V_n^q] - E[V_n^{q+1}]$, with similar calculations carried out for a bulk supercell. The latter gives us an estimate for the location of the valence band top and conduction band bottom when $q \geq 0$ and $q < 0$, respectively (see Ref. [15] for further details). Hence, for donors ($q \geq 0$) we have

$$E_d(q/q + 1) - E_v = I_d(q/q + 1) - I_m(q/q + 1),$$

whereas for acceptors ($q < 0$) we use

$$E_c - E_d(q/q + 1) = I_d(q/q + 1) - I_m(q/q + 1).$$

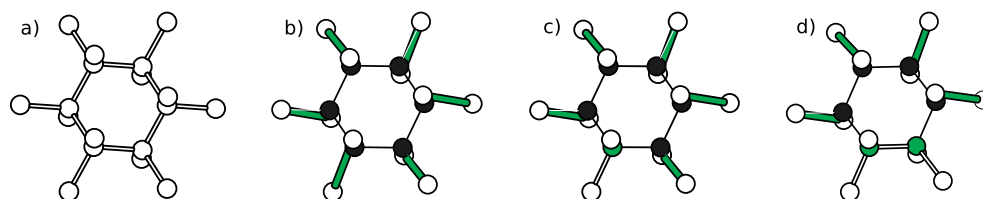


Figure 1 Atomic structure of (a) a perfect Si crystalline region, of (b) a hexavacancy V_6 , and of Part-of-Hexagonal-Ring forms of (c) a pentavacancy V_5 , and (d) a tetravacancy V_4 in Si. White and black atoms represent Si and vacant sites, whereas green atoms represent Si atoms that are added to the hexavacancy to make V_5 and V_4 .

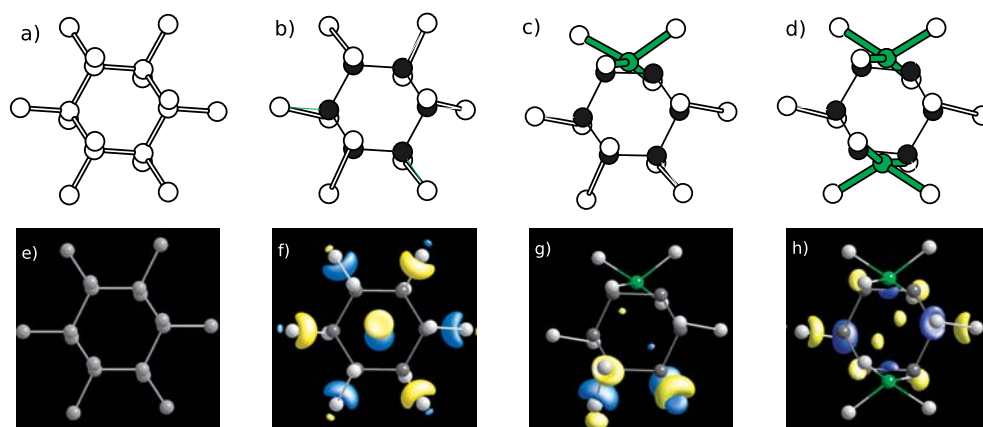


Figure 2 The top row of figures shows atomic structures of (a) a perfect Si crystalline region, of ground state structures (b) of a hexavacancy V_6 , and of Four-Fold-Coordinated forms (c) of a pentavacancy V_5 , and (d) a tetravacancy V_4 in Si. In (e)–(h) we depict identical structures combined with a rendered representation of the lowest unoccupied Kohn-Sham level of the respective vacancy defects. Yellow and blue isosurfaces represent $\psi_{T,LUKS}$ states for positive and negative values, respectively. White and black atoms represent Si and vacant sites, whereas green atoms represent Si atoms that are added to the hexavacancy to make V_5 and V_4 .

3 Results and discussion

Our calculations confirm that neutral FFC structures are stable and have lower formation energies than PHR counterparts. Accordingly, their total energy was lower than that of PHR structures by 1.25 eV and 0.62 eV for V_4 and V_5 , respectively. While PHR V_4 (with C_2 point group symmetry) was found to be a stable defect against symmetry distortion, PHR V_5 (C_{1h} point group symmetry) spontaneously relaxed to the lower energy FFC form. We know that right after irradiation only PHR V_3 has been detected by DLTS, despite neutral PHR V_3 being thermodynamically unstable against transformation to neutral FCC V_3 [13]. This must result from the non-equilibrium conditions provided by irradiation. Our results suggest that even if for kinetic reasons PHR structures are primarily formed upon irradiation, V_5 FFC defects will be readily formed even at cryogenic temperatures. The formation energy of neutral defects per unit vacancy is 2.19 eV, 1.87 eV and 1.61 eV for V_4 , V_5 and V_6 (FFC forms), respectively, demonstrating a clear drive for multivacancy aggregation.

Removing one electron from the HOKS level and placing that on a uniformly charged background *jellium* (mandatory to maintain charge neutrality of the cell) is

Table 1 Formation energies in eV for the tetra, penta and hexavacancies in FFC and PHR configurations. Calculations from Ref. [12] are also shown for comparison (braced values).

Defect	FFC	PHR
V_4	7.49 (7.26)	8.74 (8.35)
V_5	8.73 (8.42)	9.35 (9.07)
V_6		9.64 (9.43)

the standard procedure to represent a positively charged defect with a localized donor state. We found that under these conditions, supercells containing FFC V_4 and V_5 are more stable than those with PHR structures by 0.99 eV and 0.63 eV, respectively. Conversely, by adding one electron to the LUKS level (and a positive *jellium* background) to represent negatively charged states we found that cells containing FFC V_4 and V_5 are more stable than those with PHR structures by 1.05 eV and 0.62 eV, respectively. This picture is similar for doubly positive and doubly negative cells as well. We note that these results by themselves do not imply that charged V_4 and V_5 are stable. To this end we need to calculate their electrical levels (see below).

Density functional Kohn-Sham states are not one-electron states but rather eigenvectors from the Kohn-Sham equations. Despite that, their shape, localization and symmetry are often used to understand the character of donor and acceptor states. Inspection of $\psi_{\mathbf{k},\lambda}$ Kohn-Sham states at levels λ within the gap and at $\mathbf{k} = \Gamma$ allow us to understand the stability and electrical activity of these complexes. Although several levels are found within the gap, we restrict our analysis to the highest-occupied and lowest-unoccupied Kohn-Sham states ($\lambda = \text{HOKS}$ and $\lambda = \text{LUKS}$, respectively). We start describing V_6 since the other complexes inherit many of its electronic properties. While the HOKS is a valence band type state, the LUKS level [see Fig. 2(f)] is a deep a_{1u} state close to mid-gap (only 10 meV below the a_{1g} level), and is made of a linear combination of anti-bonding states between the elongated bonds shown in green in Fig. 1(b). This result is at variance with previous calculations [10,11] and questions the rather established idea that V_6 is electrically inert. Before exploring this avenue, let us examine PHR V_4 and V_5 structures. These defects have HOKS and LUKS states localized on two Si dangling bonds (symmetric and anti-symmetric states with respect to the C_2 axis and mirror plane, respectively). In V_5 this arises from a highly unstable two-fold coordinated Si atom, whereas in V_4 they are located on two three-fold coordinated Si atoms [shown in green in Figs. 1(c) and 1(d)]. States arising from the elongated bonds (with V_6 character) are closer to the band edges and should not play any role on their electrical activity. By comparing ionization energies and electron affinities of these defects with that of bulk we estimated the position of their donor and acceptor levels (see Table 2). While V_6 has first and second acceptor levels at around 0.35 eV below E_c , the Si radicals in PHR V_4 are responsible for rather deep first and second acceptor levels at about 0.7 eV below E_c . It is possible however that due to the band-gap underestimation within the LDA the depth of the calculated acceptor levels (with respect to E_c) could be overestimated. We also looked at donor levels and while these were not found in V_6 , the calculations indicate that PHR V_4 has first and second donor levels at about 0.2 eV above E_v . This result is consistent with defects possessing dangling bonds, and are close to similar levels found for PHR V_3 [13].

Now we look at FFC structures. In V_5 and V_4 , some empty elongated bond states present in V_6 are removed or displaced upwards in the gap due to the introduction of one and two four-fold coordinated Si atoms, respectively. Like in V_3 [13], states localized on FFC Si atoms of V_4 and V_5 are edging the conduction band bottom. The LUKS states, shown in Figs. 2(g) and 2(h), are mostly localized on the elongated bonds and are very similar to the LUKS level in V_6 . No filled Kohn-Sham states within the band gap and bound to (localized on) the defect were found for these structures. Electrical levels for FFC V_4 and V_5 are reported on Tab. 2 and confirm that these structures do not introduce

Table 2 Calculated electrical levels (in eV) for stable V_4 , V_5 and V_6 complexes in Si. PHR-related levels of V_4 are shown within braces. No donor levels were found for V_6 and FFC structures.

	V_4	V_5	V_6
$E_c - E(-/ =)$	0.54 (0.73)	0.47	0.34
$E_c - E(-/0)$	0.54 (0.71)	0.45	0.36
$E(0/+) - E_v$	(0.25)		
$E(+/+ +) - E_v$	(0.21)		

donor states in the gap but rather they are predicted to be double acceptors. The FFC Si atoms in V_4 and V_5 open the V_6 cage, slightly increasing the length of the elongated bonds and deepening their states. This is why both first and second acceptor levels of V_4 lie at about $E_c - 0.54$ eV and for V_5 they are predicted at about $E_c - 0.45$ eV (closer to the acceptor levels of V_6). This location is consistent with the detection in heavily irradiated Si of several DLTS levels superimposed to the $V_2(-/0)$ signal at $E_c - 0.42$ eV, and assigned to multivacancy complexes [6,7].

4 Conclusions We presented density functional calculations of structural and electronic properties of small vacancy clusters in Si. It is confirmed that neutral FFC structures of V_4 and V_5 are more stable than PHR structures. This stability order is also shown for charged complexes (from doubly positive to doubly negative charge states). While the electrical activity of PHR structures arises from under-coordinated Si radicals, the FFC forms have acceptor levels localized on elongated bonds similar to those in V_6 . Acceptor level pairs at about 0.54 eV, 0.46 eV and 0.35 eV below E_c are predicted for FFC V_4 , FFC V_5 and V_6 defects, respectively.

Acknowledgements This work was supported by Fundação para a Ciência e a Tecnologia, Portugal (FCT) under the grant PEst-C/CTM/LA0025/2011.

References

- [1] A. Dierlamm, Nucl. Instrum. Methods Phys. Res. A **624**, 396–400 (2010).
- [2] G.D. Watkins, Deep Centers in Semiconductors, 2 ed. (Gordon & Breach Science Publishers, New York, 1992), Chap. 3, p. 177.
- [3] Y.H. Lee and J.W. Corbett, Phys. Rev. B **9**, 4351–4361 (1974).
- [4] B.G. Svensson, B. Mohadjeri, A. Hallén, J.H. Svensson, and J.W. Corbett, Phys. Rev. B **43**, 2292–2298 (1991).
- [5] M. Trauwaert, J. Vanhellemont, H.E. Maes, A.V. Bavel, G. Langouche, and P. Clauws, Appl. Phys. Lett. **66**, 3056–3057 (1995).
- [6] M. Ahmed, S.J. Watts, J. Matheson, and A. Holmes-Siedle, Nucl. Instrum. Methods Phys. Res. A **457**, 588–594 (2001).
- [7] M. Moll, E. Fretwurst, M. Kuhnke, and G. Lindström, Nucl. Instrum. Methods Phys. Res. B **186**, 100–110 (2002).
- [8] G.D. Watkins and J.W. Corbett, Phys. Rev. **138**, A543–A555 (1965).

- [9] D. J. Chadi and K. J. Chang, Phys. Rev. B **38**, 1523–1525 (1988).
- [10] J. L. Hastings, S. K. Estreicher, and P. A. Fedders, Phys. Rev. B **56**, 10215–10220 (1997).
- [11] B. Hourahine, R. Jones, A. N. Safonov, S. Öberg, P. R. Briddon, and S. K. Estreicher, Phys. Rev. B **61**, 12594–12597 (2000).
- [12] D. V. Makhov and L. J. Lewis, Phys. Rev. Lett. **92**, 255504 (2004).
- [13] V. P. Markevich, A. R. Peaker, S. B. Lastovskii, L. I. Murin, J. Coutinho, V. J. B. Torres, P. R. Briddon, L. Dobaczewski, E. V. Monakhov, and B. G. Svensson, Phys. Rev. B **80**, 235207 (2009).
- [14] C. Hartwigsen, S. Goedecker, and J. Hutter, Phys. Rev. B **58**, 3641–3662 (1998).
- [15] J. Coutinho, V. J. B. Torres, R. Jones, and P. R. Briddon, Phys. Rev. B **67**, 035205 (2003).